iScience

CellPress
OPEN ACCESS

Article

Intensity and drivers of subtypes interference between seasonal influenza viruses in mainland China: A modeling study

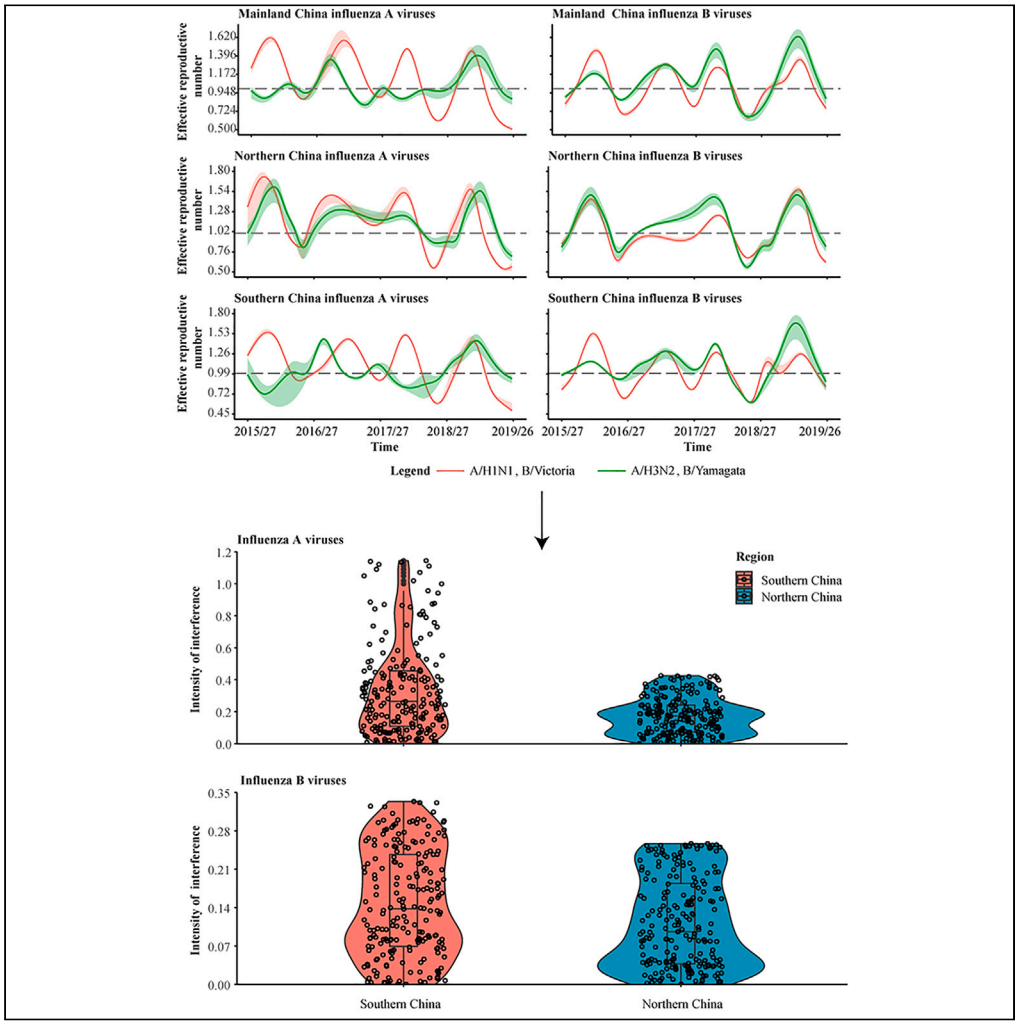

Can Chen, Mengya Yang, Yu Wang, ..., Rui Yan, Changtai Zhu, Shigui Yang

yangshigui@zju.edu.cn (S.Y.)
zct101@163.com (C.Z.)

Highlights

We first used the R_e to calculate the subtype interference between SIVs

The interference intensity between SIVs was higher in the southern China

High relative humidity facilitated subtype interference in the southern China

Chen et al., iScience *27*, 109323
March 15, 2024
https://doi.org/10.1016/j.isci.2024.109323

iScience

CellPress
OPEN ACCESS

Article

Intensity and drivers of subtypes interference between seasonal influenza viruses in mainland China: A modeling study

Can Chen,[1,4] Mengya Yang,[1,4] Yu Wang,[2,4] Daixi Jiang,[1] Yuxia Du,[1] Kexin Cao,[1] Xiaobao Zhang,[1] Xiaoyue Wu,[1] Mengsha Chen,[1] Yue You,[1] Wenkai Zhou,[1] Jiaxing Qi,[1] Rui Yan,[1] Changtai Zhu,[3,*] and Shigui Yang[1,5,*]

SUMMARY

Subtype interference has a significant impact on the epidemiological patterns of seasonal influenza viruses (SIVs). We used attributable risk percent [the absolute value of the ratio of the effective reproduction number (R_e) of different subtypes minus one] to quantify interference intensity between A/H1N1 and A/H3N2, as well as B/Victoria and B/Yamagata. The interference intensity between A/H1N1 and A/H3N2 was higher in southern China 0.26 (IQR: 0.11–0.46) than in northern China 0.17 (IQR: 0.07–0.24). Similarly, interference intensity between B/Victoria and B/Yamagata was also higher in southern China 0.14 (IQR: 0.07–0.24) than in norther China 0.10 (IQR: 0.04–0.18). High relative humidity significantly increased subtype interference, with the highest relative risk reaching 20.59 (95% CI: 6.12–69.33) in southern China. Southern China exhibited higher levels of subtype interference, particularly between A/H1N1 and A/H3N2. Higher relative humidity has a more pronounced promoting effect on subtype interference.

INTRODUCTION

The human respiratory tract provides a symbiotic environment for numerous viruses, which have the potential to infect multiple respiratory viruses simultaneously or sequentially. This can result in interference between respiratory viruses.[1] Several studies have demonstrated that this interference has a direct impact on the risk of infection for individuals and the circulation patterns within populations.[2] Currently, the A/H1N1 and A/H3N2 subtypes of influenza A virus (IAVs), along with the B/Victoria and B/Yamagata subtypes of influenza B virus (IBVs), are the dominant strains circulating in the population.[3] These strains are responsible for a significant number of infections and deaths each year.[4] The interference between A/H1N1 and A/H3N2,[5] as well as between B/Victoria and B/Yamagata,[6] is frequently observed and is even more pronounced due to their similar antigenic properties.[7,8] And, the subtype interference appears to be an important factor in influencing the magnitude, incidence, and peak of SIVs.

During the winter season of 1977–1978 in Japan, a study conducted in three schools with sequential outbreaks revealed that the percentage of children infected with the A/H1N1 virus was significantly lower among those who had been previously infected with the A/H3N2 virus compared to individuals who had not been infected with A/H3N2.[9] In the ferret experiment with IBVs, it was observed that viruses from both lineages had the ability to prevent or significantly restrict subsequent infection with a virus from the other lineage.[6] Similarly, experiments found strong cross-reactivities between H7N9 and different H7 subtypes of viruses, including H7N2, H7N3, and H7N7.[10] During the 2009–2011 A/H1N1 pdm09 virus pandemic, only the A/H1N1 pdm09 subtype was circulating, or the incidence peaks of A/H1N1 and A/H3N2 were separated in many countries, which was believed to be due to interference between the subtypes.[11,12] In Australia, it has been suggested that the subtype interference between SIVs has substantial effects on the size of epidemics and the composition of SIVs.[13] The "stronger subtypes" tend to have an advantage in maintaining a relatively high level of epidemic activity. As a result, the other subtypes may be less prevalent during the influenza season.[13]

However, there is limited quantitative evidence available to assess the subtype interference between SIVs, which is crucial for accurately understanding the circulation of SIVs.[14] In this study, our aim was to describe and quantify the intensity and drivers of subtype interference between SIVs in mainland China by using the effective reproduction number (R_e),[15] a key epidemiological parameter for measuring the transmissibility of a virus. Additionally, we also examined the potential relationships between relative humidity (RH) and the subtype interference.

[1]Department of Emergency Medicine, Second Affiliated Hospital, Department of Epidemiology and Biostatistics, School of Public Health, The Key Laboratory of Intelligent Preventive Medicine of Zhejiang Province, Zhejiang University School of Medicine, Hangzhou 310058, China
[2]College of Computer Science and Technology, Zhejiang University, Hangzhou 310058, China
[3]Department of Transfusion Medicine, Shanghai Sixth People's Hospital Affiliated to Shanghai Jiao Tong University School of Medicine, Shanghai 200233, China
[4]These authors contributed equally
[5]Lead contact
*Correspondence: yangshigui@zju.edu.cn (S.Y.), zct101@163.com (C.Z.)
https://doi.org/10.1016/j.isci.2024.109323

Table 1. The circulation of seasonal influenza viruses in Mainland China

Region	ILI%	Subtype	Positive rate (%)	Primary peak (week)
Northern	2.94	A/H1N1	9.92	9.4
Southern	3.53		8.64	10.5
Mainland China	3.3		9.14	10
Northern	2.94	A/H3N2	7.13	8.7
Southern	3.53		7.31	38.6
Mainland China	3.3		7.24	8.2
Northern	2.94	B/Victoria	3.81	17.3
Southern	3.53		4.83	20.9
Mainland China	3.3		4.43	19.3
Northern	2.94	B/Yamagata	3.91	6.5
Southern	3.53		3.25	6.0
Mainland China	3.3		3.5	6.3
Northern	2.94	SIVs	24.77	9.3
Southern	3.53		24.03	9.8
Mainland China	3.3		24.32	9.5

RESULTS

The circulation of seasonal influenza viruses in mainland China

During the period from week 27, 2015 to week 26, 2019, the proportion of influenza-like illnesses (ILI%) in outpatient visits to sentinel hospitals in mainland China was 3.30%. The positive rate of SIVs in mainland China was 24.32%. It was found to be higher in northern China (24.77%) compared to southern China (24.03%). However, the ILI% in southern China (3.53%) was higher than in northern China (2.94%) (Table 1). The regional division of the northern and southern China is detailed in Figure S1.

The primary peaks of seasonal influenza viruses circulation in mainland China

The primary peak of circulation of SIVs in mainland China occurred during weeks 9–10. It was observed that the primary peak occurred earlier in northern China (week 9.3) compared to southern China (week 9.8) (Figure 1). In northern China, the seasonality of SIVs was evident, with a typical winter epidemic peak (Figure 1). However, in southern China, the seasonality of SIV circulation became less pronounced. In addition to the primary peak, there was a secondary peak in southern China in week 39.2 and even sustained with low intensity year-round circulation (Figure 1). A hierarchical pattern of primary peaks was observed among the subtypes. The primary peak of A/H3N2 (week 8.2) occurred earlier than that of A/H1N1 (week 10.0) and the primary peak of B/Yamagata (week 6.3) was earlier than that of B/Victoria (week 19.3) (Figure 1).

The subtype interference between seasonal influenza viruses in mainland China

We used the SIB-SIRS model to analyze the circulation patterns of SIVs in mainland China. Overall, the performance of the SIB-SIRS model was relatively satisfactory (Figure S2). The estimated R_e for SIVs in mainland China was 1.04 (95% CI: 0.64–1.57). The maximum and minimum R_e values for A/H1N1 and A/H3N2 were 1.62 and 0.51, and 1.40 and 0.80, respectively. For B/Victoria and B/Yamagata, the maximum and minimum R_e values were 1.46 and 0.64, and 1.63 and 0.66, respectively (Figure 2). The dynamic pathogen spectrum is shown in the Figure S3. Sensitivity analyses were conducted for various parameters, including the contact rate, naturally acquired cross-protection, and vaccine-induced cross-protection. Among these parameters, the contact rate was found to be the main factors influencing the model (Table S1).

The intensity of subtypes interference in mainland China

In mainland China, the interference intensity between A/H1N1 and A/H3N2 was 0.26 (IQR: 0.07–0.42), which was higher than the interference intensity between B/Victoria and B/Yamagata 0.15 (IQR: 0.06–0.19) (Figure S4). In southern China, the interference intensity between A/H1N1 and A/H3N2 was higher compared to northern China, with values of 0.26 (IQR: 0.11–0.46) and 0.17 (IQR: 0.07–0.24), respectively. Similarly, the interference intensity between B/Victoria and B/Yamagata was also higher in southern China compared to northern China, with values of 0.14 (IQR: 0.07–0.24) and 0.10 (IQR: 0.04–0.18), respectively (Figure 3). The period with the maximum interference intensity also occurred in southern China (Figure 3).

The relationship between subtypes interference and relative humidity

We further investigated the association between subtype interference and RH (Figure 4). Moving from northern to southern China, as RH increases, the relative risk (RR) of subtype interference initially decreases and then significantly increases. Between A/H1N1 and A/H3N2, the RR

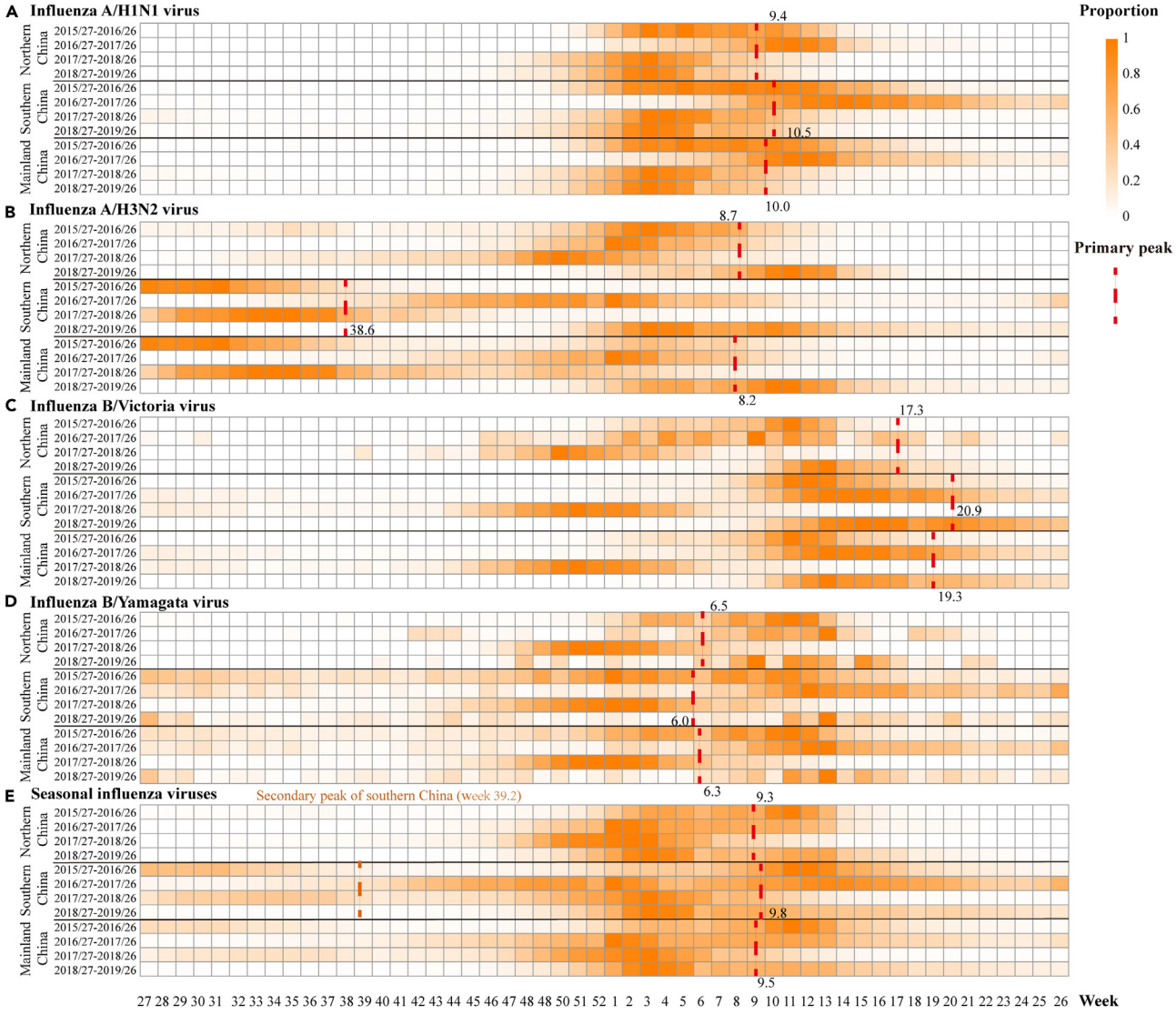

Figure 1. The primary peaks of circulation of seasonal influenza viruses in Mainland China

(A) Influenza A/H1N1 virus; (B) Influenza A/H3N2 viruses; (C) Influenza B/Victoria viruses; (D) Influenza B/Yamagata viruses; (E) Seasonal influenza viruses. Color bar represents the intensity of influenza incidence, from high (orange) to low (white). The weekly positive counts were standardized for each influenza season. Weeks with the maximum number of cases for a given influenza season were assigned the value 1. Seasonal influenza viruses comprise the sum of the four subtypes.

of subtype interference significantly increased in southern China, with the highest RR recorded at 20.59 (95% CI: 6.12–69.33), observed at 82.9% RH in southern China. In northern China, the highest RR of subtype interference was only 2.03 (95% CI: 1.32–3.13), observed at 36.6% RH. The interference between B/Victoria and B/Yamagata also exhibits a pattern of initially decreasing and then increasing. The highest RR of subtype interference between B/Victoria and B/Yamagata was 5.07 (95% CI: 1.14–22.64), observed at 86.6% RH.

DISCUSSION

In this study, we found the primary peak of SIV circulation in mainland China occurred in weeks 9–10. However, in addition to the primary peak in week 9.8, a second peak was observed in week 39.2 in southern China. The primary peaks of each subtype were distinct and separated from each other. The R_e of SIVs in mainland China was 1.04 (95% CI: 0.64–1.57). The interference intensity between A/H1N1 and A/H3N2 was 0.26 (IQR: 0.07–0.42), and between B/Victoria and B/Yamagata was 0.15 (IQR: 0.06–0.19) in mainland China. The interference intensity was higher in southern China than in northern China. High RH had a greater impact on subtype interference, especially in southern China.

The circulation of SIVs typically follows a specific pattern, starting in the northern hemisphere and gradually spreading to the southern hemisphere.[16] The timing of the primary peak is negatively correlated with latitude.[17] However, we also observed a second peak and

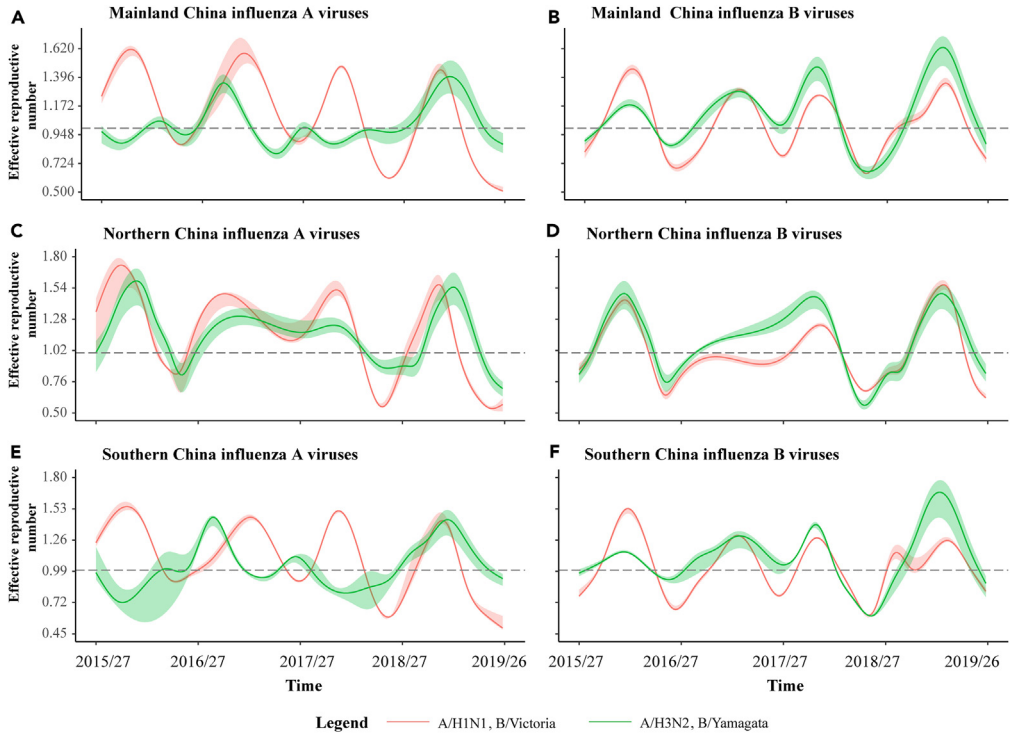

Figure 2. The Effective Reproduction Number of Seasonal Influenza Viruses

(A) Mainland China influenza A viruses; (B) Mainland China influenza B viruses; (C) Northern China influenza A viruses; (D) Northern China influenza B viruses; (E) Southern China influenza A viruses; (F) Southern China influenza B viruses.

sustained low-intensity year-round circulation of SIVs in the southern China. Generally, northern China has a temperate climate, and in southern China, known for its subtropical/tropical climate.[18] Researchers hypothesized that there might be two distinct patterns impacting the transmission of SIVs in temperate and subtropical regions. The "dry-cold mechanism" of temperate regions significantly drives influenza activity. Reduced humidity during colder seasons increases the stability of the SIVs, prolonging their survival on surfaces. Furthermore, indoor crowding during colder weather amplifies viral transmission. Consequently, influenza outbreaks in temperate regions frequently align with these climatic conditions, resulting in heightened transmission and increased influenza activity during the colder, drier months.[19] The "humid-rainy mechanism" describes the environmental conditions in tropical and subtropical regions that influence influenza seasonal patterns. In these areas, sustained high humidity and periodic rainy seasons foster an environment conducive to SIV transmission.[20] Humid tropical conditions could increase contact-based transmission by augmenting virus deposition on surfaces and prolonging virus survival within droplets.[21] Previous hypotheses on the global circulation of SIVs suggested that annual epidemic waves may propagate from Asia, where the circulation of SIVs occurs year-round.[22,23] Therefore, the year-round circulation of SIVs in southern China may play a crucial role in sustaining the circulation of SIVs in mainland China. This could potentially provide opportunities for the continuous supply of circulating SIVs to northern China.[24] Based on these findings, we recommend strengthening surveillance of SIVs in southern China. This would be more efficient for monitoring variants and identifying vaccine strain candidates for SIVs.

The early circulation of one subtype of SIVs in the population was linked to a decrease in the overall incidence of the other subtype, indicating the presence of subtype interference.[25] This phenomenon has also been observed in wild birds, where even after 15 weeks of infection with the A/H3N8 virus, they still exhibit resistance to re-infection by other subtypes of IAVs.[26] The author suggests that subtype interference may regulate the population dynamics of IAVs subtypes in nature.[26] In our study, we found that southern China exhibits higher levels of interference intensity, particularly between the A/H1N1 and A/H3N2 subtypes, which may impact the epidemiological characteristics of SIVs in this region. Additionally, we observed a hierarchical pattern of primary peaks among the subtypes, which has also been observed during SIV surveillance in other countries.[27] These phenomena have been hypothesized to be mediated by pre-existing and cross-reactive immunity, which could potentially prevent or restrict subsequent infection with a virus from the another lineage.[6,9]

Although influenza A/H1N1, A/H3N2, and B viruses have been found to circulate in various climate environments, different subtypes have shown a tendency to circulate more prominently in certain climates and seasons. Previous researches have indicated that both low and high RH are associated with an increased circulation of SIVs. It is commonly believed that low RH can sustain the viability of the influenza virus and facilitate its transmission, which has been confirmed in numerous studies.[28,29] The increased transmission of influenza in high RH appears to be due to the swelling of droplet nuclei formed when patients cough or sneeze into hygroscopic particles upon exposure to outdoor humid air, thereby facilitating the spread of the SIVs.[30] However, the effects of high RH has been observed to be more consistent in IAVs compared to

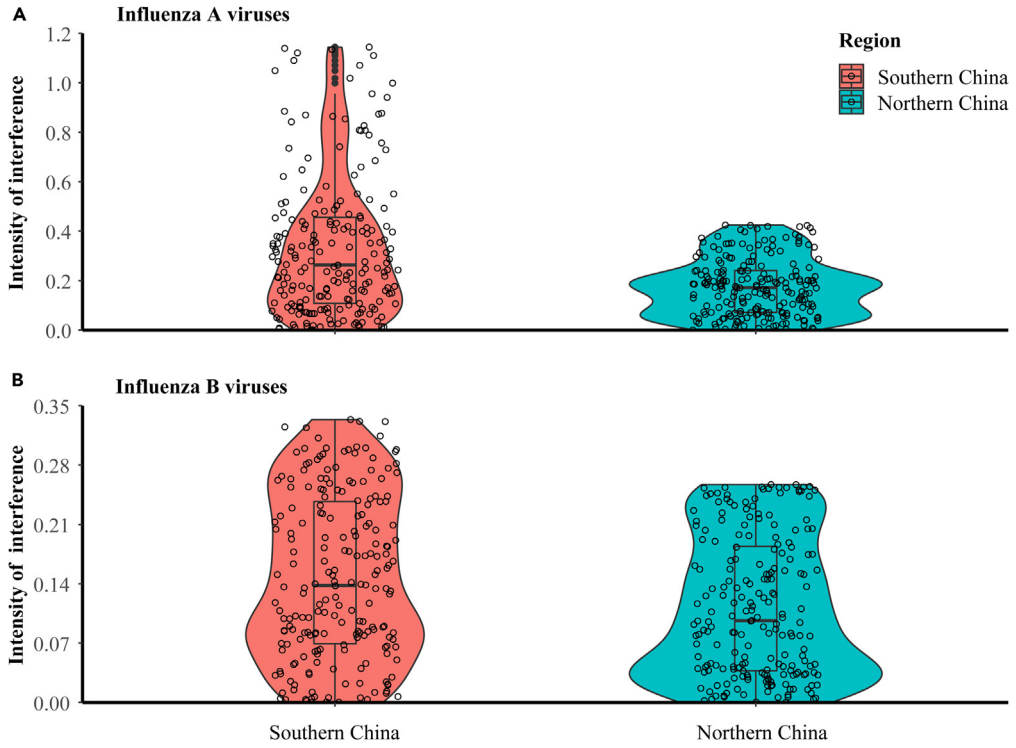

Figure 3. The Interference Intensity in Northern and Southern China

(A) Influenza A viruses; (B) Influenza B viruses.

IBVs.[31,32] Specifically, high RH has been found to increase A/H3N2 infections.[33] This may explain why high RH increases the RR of subtype interference, particularly in southern China. In this region, the overall RH is higher than in northern China, and the high RH favors the transmission of the A/H3N2 virus. Consequently, as RH increases, the RR of subtype interference between A/H1N1 and A/H3N2 also increases. In our study, we utilized epidemiological data to describe the phenomenon of subtype interference between SIVs in mainland China. Through the SIB-SIRS model, we calculated the R_e and interference intensity between subtypes. Our findings revealed that subtype interference between SIVs should not be neglected. This implies that when conducting model studies on SIVs, it is essential to consider subtype interference in order to accurately comprehend the patterns of SIVs and predict SIVs epidemics.

Limitations of the study

Our study has several limitations that should be acknowledged. Firstly, we described the phenomenon of subtype interference and calculated the overall interference intensity, without quantifying the individual contributions of pre-existing immunity and cross-immunity. In future research, we will further explore their respective contributions to the subtype interference between SIVs from various interdisciplinary perspectives. Secondly, the calculation of the weekly influenza incidence rate in our study is based on multiplying the ILI% among patients visiting sentinel hospitals by the positive rate of SIVs. However, the ILI% among outpatients may be higher than that in the general population, potentially leading to inflated estimates of the weekly influenza incidence rate and number. Thirdly, the lack of systematic surveillance data for influenza vaccination rate and vaccine effectiveness in mainland China required us to rely on data accessed through published researches. In the future, we will also concentrate on studying these fundamental parameters to provide more scientifically data. Fourth, due to the numerous parameters in our model and the limitations of our computing platform, we resorted to using the least squares method for parameter estimation. This approach may overlook the potential probabilistic distribution characteristics inherent in influenza incidence data, potentially resulting in some bias. Fifth, we assumed no cross-protection between IAVs and IBVs in our study due to the limited understanding of their interaction. This assumption may not fully capture the complexity of the interaction between these two viruses. Future studies could benefit from incorporating a more detailed understanding of the mechanism of interaction between IAVs and IBVs to improve the model.

STAR★METHODS

Detailed methods are provided in the online version of this paper and include the following:

- KEY RESOURCES TABLE
- RESOURCE AVAILABILITY

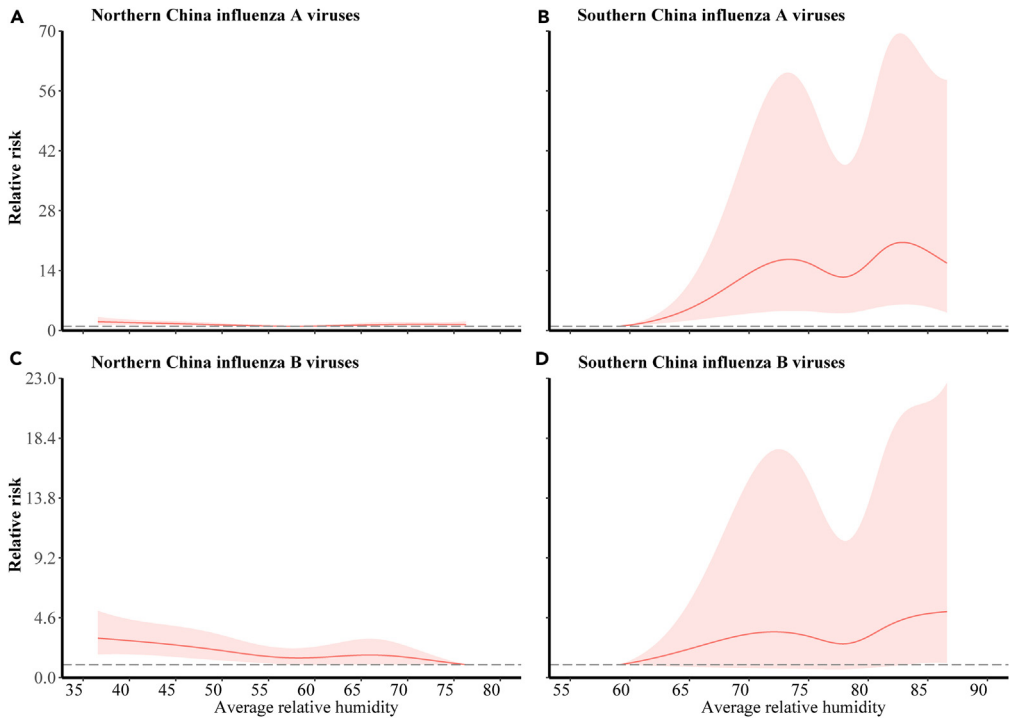

Figure 4. Effects of average relative humidity on subtype interference

(A) Effects of average relative humidity on subtype interference between A/H1N1 and A/H3N2 in northern China; (B) Effects of average relative humidity on subtype interference between A/H1N1 and A/H3N2 in southern China; (C) Effects of average relative humidity on subtype interference between B/Victoria and B/Yamagata in northern China; (D) Effects of average relative humidity on subtype interference between B/Victoria and B/Yamagata in southern China. These curves represent the changes in relative risk (RR) with variations in RH and subtype interference. When the lower 95% confidence interval of the RR is greater than 1, it indicates an increased risk of subtype interference. A higher RR value indicates a greater risk associated with subtype interference.

SUPPLEMENTAL INFORMATION

Supplemental information can be found online at https://doi.org/10.1016/j.isci.2024.109323.

ACKNOWLEDGMENTS

We would like to express our gratitude to the Chinese Center for Disease Control and Prevention and the Chinese National Influenza Center for providing access to and sharing the weekly influenza case reports.

This study was supported by grants from the National Natural Science Foundation of China (Grant Numbers: U23A20496, 82173577, 81672005); the Mega-Project of National Science and Technology for the 13th Five-Year Plan of China (Grant Numbers: 2018ZX10715-014-002).

AUTHOR CONTRIBUTIONS

S.Y. conceptualized the study. C.C., M.Y., D.J., U.D., K.C., X.Z., X.W., M.C., Y.Y., W.Z., J.Q., and R.Y. collected data. C.C. and Y.W. wrote the code for the model. C.C., S.Y., and M.Y. analyzed data. C.C., S.Y., and C.Z. checked the data and results. S.Y. and C.C. interpreted data and wrote the report. S.Y., C.Z., and C.C. revised the report from preliminary draft to submission. All authors have read and approved the article.

DECLARATION OF INTERESTS

The authors declare no competing interests.

Received: September 1, 2023
Revised: January 18, 2024
Accepted: February 20, 2024
Published: February 23, 2024

REFERENCES

1. Piret, J., and Boivin, G. (2022). Viral Interference between Respiratory Viruses. Emerg. Infect. Dis. *28*, 273–281. https://doi.org/10.3201/eid2802.211727.
2. Zhang, L., Xiao, Y., Xiang, Z., Chen, L., Wang, Y., Wang, X., Dong, X., Ren, L., and Wang, J. (2023). Statistical Analysis of Common Respiratory Viruses Reveals the Binary of Virus-Virus Interaction. Microbiol. Spectr. *11*, e0001923. https://doi.org/10.1128/spectrum.00019-23.
3. Uyeki, T.M. (2017). Ann. Intern. Med. *167*, ITC33–ITC48. https://doi.org/10.7326/AITC201709050.
4. Iuliano, A.D., Roguski, K.M., Chang, H.H., Muscatello, D.J., Palekar, R., Tempia, S., Cohen, C., Gran, J.M., Schanzer, D., Cowling, B.J., et al. (2018). Estimates of global seasonal influenza-associated respiratory mortality: a modelling study. Lancet Lond. Engl. *391*, 1285–1300. https://doi.org/10.1016/S0140-6736(17)33293-2.
5. Yang, W., Lau, E.H.Y., and Cowling, B.J. (2020). Dynamic interactions of influenza viruses in Hong Kong during 1998-2018. PLoS Comput. Biol. *16*, e1007989. https://doi.org/10.1371/journal.pcbi.1007989.
6. Laurie, K.L., Horman, W., Carolan, L.A., Chan, K.F., Layton, D., Bean, A., Vijaykrishna, D., Reading, P.C., McCaw, J.M., and Barr, I.G. (2018). Evidence for Viral Interference and Cross-reactive Protective Immunity Between Influenza B Virus Lineages. J. Infect. Dis. *217*, 548–559. https://doi.org/10.1093/infdis/jix509.
7. Ferguson, N.M., Galvani, A.P., and Bush, R.M. (2003). Ecological and immunological determinants of influenza evolution. Nature *422*, 428–433. https://doi.org/10.1038/nature01509.
8. Susi, H., Barrès, B., Vale, P.F., and Laine, A.-L. (2015). Co-infection alters population dynamics of infectious disease. Nat. Commun. *6*, 5975. https://doi.org/10.1038/ncomms6975.
9. Sonoguchi, T., Naito, H., Hara, M., Takeuchi, Y., and Fukumi, H. (1985). Cross-subtype protection in humans during sequential, overlapping, and/or concurrent epidemics caused by H3N2 and H1N1 influenza viruses. J. Infect. Dis. *151*, 81–88. https://doi.org/10.1093/infdis/151.1.81.
10. Guo, L., Wang, D., Zhou, H., Wu, C., Gao, X., Xiao, Y., Ren, L., Paranhos-Baccalà, G., Shu, Y., Jin, Q., and Wang, J. (2016). Cross-reactivity between avian influenza A (H7N9) virus and divergent H7 subtypic- and heterosubtypic influenza A viruses. Sci. Rep. *6*, 22045. https://doi.org/10.1038/srep22045.
11. Van Kerkhove, M.D., and Mounts, A.W. (2011). 2009 versus 2010 comparison of influenza activity in southern hemisphere temperate countries. Influenza Other Respir. Viruses *5*, 375–379. https://doi.org/10.1111/j.1750-2659.2011.00241.x.
12. Yang, Y., Wang, Z., Ren, L., Wang, W., Vernet, G., Paranhos-Baccalà, G., Jin, Q., and Wang, J. (2012). Influenza A/H1N1 2009 Pandemic and Respiratory Virus Infections, Beijing, 2009-2010. PLoS One *7*, e45807. https://doi.org/10.1371/journal.pone.0045807.
13. Lam, E.K.S., Morris, D.H., Hurt, A.C., Barr, I.G., and Russell, C.A. (2020). The impact of climate and antigenic evolution on seasonal influenza virus epidemics in Australia. Nat. Commun. *11*, 2741. https://doi.org/10.1038/s41467-020-16545-6.
14. Opatowski, L., Baguelin, M., and Eggo, R.M. (2018). Influenza interaction with cocirculating pathogens and its impact on surveillance, pathogenesis, and epidemic profile: A key role for mathematical modelling. PLoS Pathog. *14*, e1006770. https://doi.org/10.1371/journal.ppat.1006770.
15. Chen, X., Wang, W., Qin, Y., Zou, J., and Yu, H. (2022). Global Epidemiology of Human Infections With Variant Influenza Viruses, 1959-2021: A Descriptive Study. Clin. Infect. Dis. *75*, 1315–1323. https://doi.org/10.1093/cid/ciac168.
16. Li, Y., Reeves, R.M., Wang, X., Bassat, Q., Brooks, W.A., Cohen, C., Moore, D.P., Nunes, M., Rath, B., Campbell, H., et al. (2019). Global patterns in monthly activity of influenza virus, respiratory syncytial virus, parainfluenza virus, and metapneumovirus: a systematic analysis. Lancet. Glob. Health *7*, e1031–e1045. https://doi.org/10.1016/S2214-109X(19)30264-5.
17. Chen, C., Jiang, D., Yan, D., Pi, L., Zhang, X., Du, Y., Liu, X., Yang, M., Zhou, Y., Ding, C., Lan, L., and Yang, S. (2023). The Global Region-specific Epidemiologic Characteristics of Influenza: World Health Organization FluNet Data from 1996 to 2021. Int. J. Infect. Dis. *129*, 118–124.
18. Shu, Y.-L., Fang, L.-Q., de Vlas, S.J., Gao, Y., Richardus, J.H., and Cao, W.-C. (2010). Dual seasonal patterns for influenza, China. Emerg. Infect. Dis. *16*, 725–726. https://doi.org/10.3201/eid1604.091578.
19. Dave, K., and Lee, P.C. (2019). Global Geographical and Temporal Patterns of Seasonal Influenza and Associated Climatic Factors. Epidemiol. Rev. *41*, 51–68. https://doi.org/10.1093/epirev/mxz008.
20. Yuan, H., Kramer, S.C., Lau, E.H.Y., Cowling, B.J., and Yang, W. (2021). Modeling influenza seasonality in the tropics and subtropics. PLoS Comput. Biol. *17*, e1009050. https://doi.org/10.1371/journal.pcbi.1009050.
21. Paynter, S. (2015). Humidity and respiratory virus transmission in tropical and temperate settings. Epidemiol. Infect. *143*, 1110–1118. https://doi.org/10.1017/S0950268814002702.
22. Petrova, V.N., and Russell, C.A. (2018). The evolution of seasonal influenza viruses. Nat. Rev. Microbiol. *16*, 47–60. https://doi.org/10.1038/nrmicro.2017.118.
23. Russell, C.A., Jones, T.C., Barr, I.G., Cox, N.J., Garten, R.J., Gregory, V., Gust, I.D., Hampson, A.W., Hay, A.J., Hurt, A.C., et al. (2008). The global circulation of seasonal influenza A (H3N2) viruses. Science *320*, 340–346. https://doi.org/10.1126/science.1154137.
24. Lei, H., Yang, L., Wang, G., Zhang, C., Xin, Y., Sun, Q., Zhang, B., Chen, T., Yang, J., Huang, W., et al. (2022). Transmission Patterns of Seasonal Influenza in China between 2010 and 2018. Viruses *14*, 2063. https://doi.org/10.3390/v14092063.
25. Goldstein, E., Cobey, S., Takahashi, S., Miller, J.C., and Lipsitch, M. (2011). Predicting the epidemic sizes of influenza A/H1N1, A/H3N2, and B: a statistical method. PLoS Med. *8*, e1001051. https://doi.org/10.1371/journal.pmed.1001051.
26. Latorre-Margalef, N., Brown, J.D., Fojtik, A., Poulson, R.L., Carter, D., Franca, M., and Stallknecht, D.E. (2017). Competition between influenza A virus subtypes through heterosubtypic immunity modulates re-infection and antibody dynamics in the mallard duck. PLoS Pathog. *13*, e1006419. https://doi.org/10.1371/journal.ppat.1006419.
27. Suzuki, A., Mizumoto, K., Akhmetzhanov, A.R., and Nishiura, H. (2019). Interaction Among Influenza Viruses A/H1N1, A/H3N2, and B in Japan. Int. J. Environ. Res. Public Health *16*, 4179. https://doi.org/10.3390/ijerph16214179.
28. Lowen, A.C., Mubareka, S., Steel, J., and Palese, P. (2007). Influenza virus transmission is dependent on relative humidity and temperature. PLoS Pathog. *3*, 1470–1476. https://doi.org/10.1371/journal.ppat.0030151.
29. Yang, W., and Marr, L.C. (2011). Dynamics of airborne influenza A viruses indoors and dependence on humidity. PLoS One *6*, e21481. https://doi.org/10.1371/journal.pone.0021481.
30. Wu, Q., He, J., Zhang, W.-Y., Zhao, K.-F., Jin, J., Yu, J.-L., Chen, Q.-Q., Hou, S., Zhu, M., Xu, Z., and Pan, H.F. (2021). The contrasting relationships of relative humidity with influenza A and B in a humid subtropical region. Environ. Sci. Pollut. Res. Int. *28*, 36828–36836. https://doi.org/10.1007/s11356-021-13107-1.
31. Chong, K.C., Lee, T.C., Bialasiewicz, S., Chen, J., Smith, D.W., Choy, W.S.C., Krajden, M., Jalal, H., Jennings, L., Alexander, B., et al. (2020). Association between meteorological variations and activities of influenza A and B across different climate zones: a multi-region modelling analysis across the globe. J. Infect. *80*, 84–98. https://doi.org/10.1016/j.jinf.2019.09.013.
32. Lei, H., Yang, M., Dong, Z., Hu, K., Chen, T., Yang, L., Zhang, N., Duan, X., Yang, S., Wang, D., et al. (2023). Indoor relative humidity

shapes influenza seasonality in temperate and subtropical climates in China. Int. J. Infect. Dis. *126*, 54–63. https://doi.org/10.1016/j.ijid.2022.11.023.

33. Zhou, L., Yang, H., Pan, W., Xu, J., Feng, Y., Zhang, W., Shao, Z., Li, T., Li, S., Huang, T., et al. (2022). Association between meteorological factors and the epidemics of influenza (sub)types in a subtropical basin of Southwest China. Epidemics *41*, 100650. https://doi.org/10.1016/j.epidem.2022.100650.
34. Lei, H., Xu, M., Wang, X., Xie, Y., Du, X., Chen, T., Yang, L., Wang, D., and Shu, Y. (2020). Nonpharmaceutical Interventions Used to Control COVID-19 Reduced Seasonal Influenza Transmission in China. J. Infect. Dis. *222*, 1780–1783. https://doi.org/10.1093/infdis/jiaa570.
35. Alonso, W.J., Yu, C., Viboud, C., Richard, S.A., Schuck-Paim, C., Simonsen, L., Mello, W.A., and Miller, M.A. (2015). A global map of hemispheric influenza vaccine recommendations based on local patterns of viral circulation. Sci. Rep. *5*, 17214. https://doi.org/10.1038/srep17214.
36. Sachak-Patwa, R., Byrne, H.M., and Thompson, R.N. (2021). Accounting for cross-immunity can improve forecast accuracy during influenza epidemics. Epidemics *34*, 100432. https://doi.org/10.1016/j.epidem.2020.100432.
37. Liu, H., Zhang, J., Cai, J., Deng, X., Peng, C., Chen, X., Yang, J., Wu, Q., Chen, X., Chen, Z., et al. (2022). Investigating vaccine-induced immunity and its effect in mitigating SARS-CoV-2 epidemics in China. BMC Med. *20*, 37. https://doi.org/10.1186/s12916-022-02243-1.
38. Chen, C., Liu, X., Yan, D., Zhou, Y., Ding, C., Chen, L., Lan, L., Huang, C., Jiang, D., Zhang, X., et al. (2022). Global Influenza Vaccination Rates and Factors Associated with Influenza Vaccination. Int. J. Infect. Dis. *125*, 153–163. https://doi.org/10.1016/j.ijid.2022.10.038.
39. Kohler, I., Scherrer, A.U., Zagordi, O., Bianchi, M., Wyrzucki, A., Steck, M., Ledergerber, B., Günthard, H.F., and Hangartner, L. (2014). Prevalence and predictors for homo- and heterosubtypic antibodies against influenza a virus. Clin. Infect. Dis. *59*, 1386–1393. https://doi.org/10.1093/cid/ciu660.
40. Lei, H., Jiang, H., Zhang, N., Duan, X., Chen, T., Yang, L., Wang, D., and Shu, Y. (2021). Increased urbanization reduced the effectiveness of school closures on seasonal influenza epidemics in China. Infect. Dis. Poverty *10*, 127. https://doi.org/10.1186/s40249-021-00911-7.
41. Ho, S.H., He, D., and Eftimie, R. (2019). Mathematical models of transmission dynamics and vaccine strategies in Hong Kong during the 2017-2018 winter influenza season. J. Theor. Biol. *476*, 74–94. https://doi.org/10.1016/j.jtbi.2019.05.013.
42. 11.4 Bootstrapping and Bagging | Forecasting: Principles and Practice (2nd ed)
43. Bubar, K.M., Reinholt, K., Kissler, S.M., Lipsitch, M., Cobey, S., Grad, Y.H., and Larremore, D.B. (2021). Model-informed COVID-19 vaccine prioritization strategies by age and serostatus. Science *371*, 916–921. https://doi.org/10.1126/science.abe6959.
44. Gauthier, J., Wu, Q.V., and Gooley, T.A. (2020). Cubic splines to model relationships between continuous variables and outcomes: a guide for clinicians. Bone Marrow Transplant. *55*, 675–680. https://doi.org/10.1038/s41409-019-0679-x.
45. Wang, D., Lei, H., Wang, D., Shu, Y., and Xiao, S. (2023). Association between Temperature and Influenza Activity across Different Regions of China during 2010-2017. Viruses *15*, 594. https://doi.org/10.3390/v15030594.
46. Qi, L., Gao, Y., Yang, J., Ding, X.-B., Xiong, Y., Su, K., Liu, T., Li, Q., Tang, W.-G., and Liu, Q.-Y. (2020). The burden of influenza and pneumonia mortality attributable to absolute humidity among elderly people in Chongqing, China, 2012-2018. Sci. Total Environ. *716*, 136682. https://doi.org/10.1016/j.scitotenv.2020.136682.
47. Alonso, W.J., and McCormick, B.J.J. (2012). EPIPOI: a user-friendly analytical tool for the extraction and visualization of temporal parameters from epidemiological time series. BMC Publ. Health *12*, 982. https://doi.org/10.1186/1471-2458-12-982.

STAR★METHODS

KEY RESOURCES TABLE

REAGENT or RESOURCE	SOURCE	IDENTIFIER
Deposited data		
Influenza Surveillance Data	Chinese National Influenza Center	https://ivdc.chinacdc.cn/cnic/
Meteorological Data	China meteorological data sharing service system	www.data.cma.cn
Software and algorithms		
R	https://www.r-project.org/	N/A
Python	https://www.python.org/	N/A
EPIPOI	http://www.epipoi.info/about-epipoi/	N/A

RESOURCE AVAILABILITY

Lead contact

Further information and requests for resources and reagents should be directed to and will be fulfilled by the lead contact, Prof. Shigui Yang (yangshigui@zju.edu.cn).

Materials availability

The study did not generate any new materials.

Data and code availability

- All data used in this paper will be shared by the lead contact Shigui Yang (yangshigui@zju.edu.cn) upon request.
- The code of model in this paper will be shared by the lead contact Shigui Yang (yangshigui@zju.edu.cn) upon request.
- Any additional information required to reanalyze the data reported in this paper is available from the lead contact Shigui Yang (yangshigui@zju.edu.cn) upon request.

METHOD DETAILS

Influenza surveillance data and meteorological data in mainland China

In this study, we utilized influenza surveillance data and meteorological data from Mainland China. The weekly influenza surveillance data, spanning from week 27, 2015 to week 26, 2019, were obtained from the Chinese National Influenza Center. The extracted data included the number of laboratory-confirmed cases for A/H1N1, A/H3N2, unsubtyped IAVs, B/Victoria, B/Yamagata, and unsubtyped IBVs, as well as the number of samples tested, outpatient visits, and cases of ILI reported by sentinel hospitals. To estimate the "weekly incidence rate", we multiplied the proportion of ILI cases among outpatient visits by the virus detection positive rate.[25,34] However, due to the presence of numerous unsubtyped IAVs and IBVs, calculating the positive rate for specific subtypes could introduce bias in estimating the weekly incidence rate. To address this issue, we assigned the weekly number of positive samples for unsubtyped IAVs and IBVs to their respective subtypes based on the proportion of weekly A/H1N1, A/H3N2, B/Victoria, and B/Yamagata viruses. Additionally, we obtained daily data on relative humidity (RH, %) from 839 climate monitor stations across mainland China for the period from 2015 to 2019 through the China meteorological data sharing service system (www.data.cma.cn). To calculate the average weekly meteorological data, we aggregated the daily data.

The primary peaks of seasonal influenza viruses in mainland China

We determined the timing of the primary and second peaks of SIVs by using the data of test positive rate. We first used the quadratic polynomial to detrended each time series data of SIVs to obtain the series of trend and seasonality. And then, the timing of primary and second peaks in the series of trend and seasonality was identified, when the maximum and secondary intensity of disease burden typically occurred.[35]

Subtypes Interference Based Susceptible-Infected-Recovered-Susceptible model

In our study, subtypes interference refers to a phenomenon in which the transmission of one subtype hinders the transmission process of another subtype at the same time point. We have developed a Subtypes Interference Based Susceptible-Infected-Recovered-Susceptible (SIB-SIRS) model (Figure S5) to simulate the epidemics of SIVs (including A/H1N1, A/H3N2, B/Victoria, and B/Yamagata) in mainland China,

encompassing both northern and southern regions. Our SIB-SIRS model is based on the following assumptions: 1) cross-protection exists between A/H1N1 and A/H3N2, as well as between B/Victoria and B/Yamagata;[36] 2) there is no cross-protection between IAVs and IBVs; 3) The effectiveness of influenza vaccines follows an "all-or-nothing" principle.[37] Due to the lack of comprehensive surveillance data on influenza vaccination rates (IVR) and vaccine effectiveness (VE) in mainland China, we utilized the average annual IVR (10.02%, 95% CI: 7.10%–13.37%) across three age groups: 0-14 years old (28.41%), 15-59 years old (9.14%), and 60+ years old (13.06%).[38] The VE in mainland China was referred to United States Centers for Disease Control and Prevention (Table S2).

For the IAVs, $S^{u}_{H1}S^{u}_{H3}$ are susceptible for both A/H1N1 and A/H3N2; $I^{u}_{H1}S^{u}_{H3}$ are infected with A/H1N1 but remain susceptible for A/H3N2; $R^{u}_{H1}S^{u}_{H3}$ have recovered for A/H1N1 but remain susceptible for A/H3N2; $R^{u}_{H1}I^{u}_{H3}$ have recovered for A/H1N1 but infected with A/H3N2; $I^{u}_{H3}S^{u}_{H1}$ are infected with A/H3N2 but remain susceptible for A/H1N1; $R^{u}_{H3}S^{u}_{H1}$ have recovered for A/H3N2 but remain susceptible for A/H1N1; $R^{u}_{H3}I^{u}_{H1}$ have recovered for A/H3N2 but infected with A/H1N1; $R^{u}_{H3}R^{u}_{H1}$ have recovered for both A/H3N2 and A/H1N1; $R^{v}_{H3}R^{v}_{H1}$ have received influenza vaccination and are immunized against both A/H1N1 and A/H3N2. Total population (N) = $S^{u}_{H1}S^{u}_{H3}$ + $I^{u}_{H1}S^{u}_{H3}$ + $R^{u}_{H1}S^{u}_{H3}$ + $R^{u}_{H1}I^{u}_{H3}$ + $I^{u}_{H3}S^{u}_{H1}$ + $R^{u}_{H3}S^{u}_{H1}$ + $R^{u}_{H3}I^{u}_{H1}$ + $R^{u}_{H3}R^{u}_{H1}$ + $R^{v}_{H3}R^{v}_{H1}$. The model of IBVs is similar to IAVs. A/H1N1 and A/H3N2 are equivalent to B/Victoria (B_{vic}) and B/Yamagata (B_{Ya}). Since quadrivalent influenza vaccine was only marketed in mainland China in 2019, we assumed that public received trivalent influenza vaccine (TIV) from week 27, 2015 to week 26, 2019. In mainland China, there is no immune component for B/Yamagata virus in TIV, therefore, those who are vaccinated with TIV would remain susceptible to B/Yamagata virus, but they will have part of cross-protection against B/Yamagata due to immune component for B/Victoria virus (vaccine-induced cross-protection).[39]

In our model, i = 1 corresponds to children aged 0-14, i = 2 corresponds to individuals aged 15-59, and i = 3 corresponds to older adults aged > 60; The parameter $\lambda(t)$ is defined as $\lambda(t) = \beta(t)C\delta_i$. Here, $\beta(t)$ represents the transmission efficiency per contact at time t, C represents the contact mixing rates between an infected individual and a susceptible individual; The parameter δ_i represents the age group susceptibility to SIVs. According to a previous study, the values of δ_1, δ_2, and δ_3 were taken as 2, 1, and 2, respectively, representing a ratio of 2:1:2 for susceptibility among the different age groups;[40] We also considered the impact of climates on influenza transmission by incorporating it via the function $\beta(t) = a(1 + b\ \sin(2\pi t/52 + c))$. Here, b represents the relative contribution of climates on influenza transmission efficiency;[40] L represents the duration of immunity, and $1/\gamma$ represents the infectious period. P1 and P2 denote naturally acquired cross-immunity and vaccine-induced cross-immunity, respectively. In our model, the simulation time was set to 52 weeks. We also take into account natural birth and death processes. The initial value of the infected population was determined by the number of individuals infected with each subtype during the first week.

We combined the bootstrap method with the least squares method to infer the unknown parameters (a, b, c, and δ).[41] Since the time-series properties of the incidence data of SIVs, we first applied a Box-Cox transformation to the data. Then, we utilized seasonal and trend decomposition to decompose the data into its constituent parts, including the trend, seasonal, and random components. The random components were then resampled using the 'blocked bootstrap' method. These resampled random components were combined with the original trend and seasonal components to generate 999 new virtual time series data that closely resemble the observed data after the Box-Cox transformation.[42] We combined the observed data with the 999 generated virtual time series data to obtain a total of 1,000 incidence data for the SIVs. The SIB-SIRS model was then used to fit these data. In each simulation, we utilized the least squares method to estimate the unknown parameters of the model. After obtaining all the parameters (Table S3), we used the next-generation matrix (NG) method[43] to calculate the effective reproductive number (R_e). We define NG as:

$$M = \beta * C * D^{43}$$

where, β represents the probability of a successful transmission given contact with an infectious individual; C denotes the contact matrix, and D representing the infectious period. The effective reproduction number, R_e, is the absolute value of the dominant eigenvalue of M. In 1,000 simulations, we calculated R_e 1,000 times per week and we used the restricted cubic spline[44] to predict the R_e and its 95% confidence interval between week 27, 2015 and week 26, 2019.

The relationship between subtypes interference and meteorologic factors

A distributed lag nonlinear model was utilized to analyze the exposure-lag response of RH on subtypes interference.[45] The formula for RH model is: $Log[E(Yt)] = \alpha + \beta\ (RH_{t,l},\ lag = 2) + ns\ (Time_t)$. Where Y_t denotes the interference intensity at time t. α is the intercept; $RH_{t,l}$ represented the "cross-basis" function[46] for the RH; β denote the corresponding regression coefficients of RH. The degrees of freedom for these variables were set to 3. The function ns denotes a natural cubic spline function. $Time_t$ represents the long-term trend.

QUANTIFICATION AND STATISTICAL ANALYSIS

We used attributable risk percent [the absolute value of ratio of the R_e of different subtypes minus one] to quantify interference intensity between A/H1N1 and A/H3N2, as well as B/Victoria and B/Yamagata.

We utilized R (version 3.6.1), Python (version 3.7.4), and EPIPOI[47] for data cleaning and analysis.